Journal of Applied Polymer Science

# Application of the thermal energy storage concept to novel epoxy-short carbon fiber composites

**A. Dorigato**,[1,2] **G. Fredi**,[1] **A. Pegoretti**[1,2]
[1]Department of Industrial Engineering, University of Trento, Via Sommarive 9, 38123, Trento, Italy
[2]National Interuniversity Consortium of Materials Science and Technology (INSTM), Via G.Giusti 9, 50121, Florence, Italy
Correspondence to: A. Dorigato (E-mail: andrea.dorigato@unitn.it) and A. Pegoretti (E-mail: alessandro.pegoretti@unitn.it)

**ABSTRACT:** For the first time, multifunctional epoxy–short carbon fiber reinforced composites suitable for thermal energy storage technology were developed. Paraffin microcapsules (MC) and short carbon fibers (CFs) were added at different relative amounts to an epoxy matrix, and the microstructural and thermomechanical properties of the resulting materials were investigated. Scanning electron microscopy images of the composites showed a uniform distribution of the capsules within the matrix, with a rather good interfacial adhesion, while the increase in the polymer viscosity at elevated CF and MC amounts caused an increase in the void content. Differential scanning calorimetry tests revealed that melting enthalpy values (up to 60 J/g) can be obtained at high MC concentrations. The mixing and thermal curing of the composites did not lead to breakage of the capsules and to the consequent leakage of the paraffin out of the epoxy matrix. The thermal stability of the prepared composites is not negatively affected by the MC addition, and the temperatures at which the thermal degradation process begins were far above the curing or service temperature of the composites. Flexural and impact tests highlighted that the presence of MC reduces the mechanical properties of the samples, while CF positively contributes to retaining the original stiffness and mechanical resistance. © 2019 Wiley Periodicals, Inc. J. Appl. Polym. Sci. **2019**, *136*, 47434.

**KEYWORDS:** differential scanning calorimetry; mechanical properties; microscopy

Received 21 August 2018; accepted 28 November 2018
**DOI: 10.1002/app.47434**

## INTRODUCTION

It is well known that thermal energy storage (TES) technology is a tool for more efficient use of thermal energy. In fact, thanks to the possibility of storing heat and releasing it when needed, it is possible to couple energy availability and demand.[1–3] TES technology can be applied in a wide variety of sectors, ranging from power-generation plants[4,5] to buildings with low energy demands,[6,7] where the demand for thermal energy may considerably fluctuate even during the same day.[8] Thermal energy can be stored and released in three main ways, namely as sensible heat (due to temperature variations within the material), through thermochemical reactions, or as latent heat, that is, by using phase change materials (PCMs). PCMs are subjected to reversible solid/solid or solid/liquid phase transitions and can be classified as organic, inorganic, or eutectic.[9] The advantages associated with the use of PCMs mainly consist of the possibility of storing a large amount of thermal energy per unit mass in a very narrow temperature range, with very limited volume variations.[10] Among organic PCMs, paraffin waxes are the most widely used in TES applications,[11,12] especially because of their elevated energy density, narrow working temperature range, versatility, lightness, and cheapness.[13,14] Thanks to these peculiar features, TES systems based on PCMs can be successfully applied in buildings,[15,16] smart textiles,[17] solar plants,[18] hot/cold water storage,[19] and the thermal regulation of electronic devices.[20] The most serious drawbacks of organic PCMs are their intrinsic limited thermal conductivity and the need for confinement to avoid leakage when above their melting point.[21] The latter problem is nowadays addressed with two main techniques. The first method is the so-called "shape stabilization," which consists of the confinement of the PCM with a polymer matrix,[22–25] a nanostructured layered material,[20,26] or a percolative network constituted of an inorganic nanofiller.[27–29] If a metallic or a carbon-based material is used as stabilizing agent, it is also possible to increase the thermal conductivity of the system.[27,30,31] The second possibility is the encapsulation of the PCMs in organic or inorganic shells, which also protect the PCM from the external environment and enhance its thermal stability.[32–34]

In most technological TES applications, thermal energy storage functions are devolved to a specific added module containing PCMs. However, it could also be interesting to develop a multifunctional material capable of effectively contributing to the thermal management. In this framework, composite materials constituted of two or more phases with different properties[35–39] could be designed to combine load-bearing properties and functional capabilities. Lightweight polymer matrix composites coupling structural or semistructural functions and TES capability could be successfully applied where weight and volume savings need to be combined with precise temperature control. Even though several papers have recently been published on encapsulated and shape-stabilized PCMs in various polymer matrixes,[40–43] only a few papers dealing with the development of structural composites with TES capability can be found. The major parts of the scientific reports deal with sandwich structures for thermal management with[20] or without[44,45] the introduction of a PCM. To our knowledge, only Yoo and coworkers[46,47] studied the thermomechanical and viscoelastic properties of a glass fiber–epoxy composite with microencapsulated PCM. Our group has recently developed multifunctional epoxy–carbon fiber composites containing various percentages of a paraffin shape stabilized with carbon nanotubes (CNTs).[48,49] The thermomechanical behavior of a polyamide 12 (PA12)–glass fiber thermoplastic composite with TES functions was also studied.[9] In all these works, it was demonstrated that the introduction of the TES capability comes at the expense of the thermomechanical stability of the system.

Short carbon fibers are one of the most widely used reinforcements to improve the mechanical and tribological performance of polymers. Compared to continuous fiber reinforced composites, short fiber reinforced composites (SFRCs) combine easier processability with a low manufacturing cost. With the use of SFRCs, it is therefore possible to fill the mechanical property gap between the continuous-fiber laminates used as primary structures and the unreinforced polymers used for nonstructural applications.[50] This is the main reason why in the last few years the use of SFRCs has grown rapidly in various engineering applications, especially in the automotive and mechanical engineering sectors.[51] To the best of our knowledge, no papers dealing with short fiber reinforced thermosetting composites with thermal energy storage/release capability can be found in the open literature. Therefore, the objective of the present paper is to present a systematic investigation of the main physical properties of multifunctional epoxy–short carbon fiber reinforced composites suitable for thermal energy storage technology. To this aim, paraffin microcapsules (MC) having a melting temperature of about 43°C were dispersed at different concentrations in an epoxy matrix, keeping a constant amount of carbon fiber (CF). In another series of samples, a constant MC loading was utilized to prepare samples with different CF content. The subsequent characterization aimed to investigate the role played by the addition of MC and CF on the microstructural, thermal, and mechanical behavior of the prepared materials.

## EXPERIMENTAL

### Materials

The epoxy base Elan-tech EC157 (density = 1.15 g/cm$^3$, viscosity at 25°C = 550 mPa s) and the hardener Elan-tech W342 (density = 0.95 g/cm$^3$, viscosity at 25°C = 50 mPa s) were kindly provided by Elantas Europe Srl (Collecchio, Italy). Short carbon fibers, Panex 35, supplied by Zoltek (Saint Louis, MO), having a density of 1.78 g/cm$^3$, a diameter of 7 μm, and a length of about 0.2 mm, were used as reinforcement. Microencapsulated PCM Microtek MPCM43D was purchased from Microtek Laboratories (Dayton, OH). In these microcapsules, the PCM phase consists of a paraffin wax with a melting temperature of 43°C, and it is encapsulated inside a stable melamine–formaldehyde shell, which accounts for 10–15% of the mass. These microcapsules are characterized by a mean diameter of 17–20 μm, and the melting enthalpy declared by the producer is 190–200 J/g. All materials were used as received.

### Sample Preparation

The epoxy base and the hardener were mixed at a constant weight ratio of 100:30 together with the CF and MC at different relative concentrations by using a mechanical mixer at 1000 rpm for 5 min. The resulting mixtures were then degassed under vacuum and poured into silicone molds. The samples were then cured at ambient temperature for 24 h, followed by a postcuring treatment of 10 h at 100°C. In this way, neat epoxy (EP) and composite samples with various CF and MC concentrations were prepared. The flow chart representing the preparation of the samples is given in Figure 1, and the list of the prepared formulations is reported in Table I. A first series of samples was prepared by keeping a constant CF amount of 10 wt % and varying the MC content from 5 wt % up to 30 wt % of the total matrix (epoxy + MC) fraction. In a second group of samples, the MC amount was kept constant at 20 wt % of the total matrix fraction and the reinforcement concentration was varied between 5 wt % and 20 wt %.

### Characterization

The experimental density of the matrixes and of the composites was measured according to the standard ASTM D792 by a liquid displacement method in ethanol,[52] using a Gibertini (Milano, Italy) E42 analytical balance. Moreover, a theoretical density could be obtained by knowing the density of the individual constituents and assuming a mixture rule. The comparison between the experimental and theoretical density led to an estimation of the void volume fraction, and subsequently of the volume distribution of fibers and matrix.

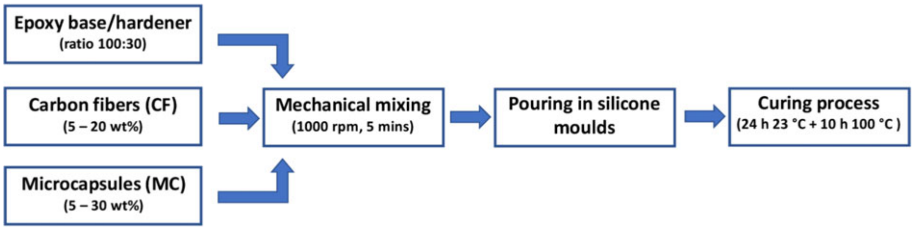

**Figure 1.** Flow chart representing the preparation of the composite samples. [Color figure can be viewed at wileyonlinelibrary.com]

**Table I.** Prepared Samples with Nominal Weight Percentages of the Constituents

| Sample | Epoxy (wt %) | Microcapsules (wt %) | Carbon fibers (wt %) |
|---|---|---|---|
| EP | 100.0 | 0.0 | 0.0 |
| MC | 0.0 | 100.0 | 0.0 |
| EP-CF10 | 90.0 | 0.0 | 10.0 |
| EP-MC5-CF10 | 85.5 | 4.5 | 10.0 |
| EP-MC15-CF10 | 76.5 | 13.5 | 10.0 |
| EP-MC30-CF10 | 63.0 | 27.0 | 10.0 |
| EP-MC20 | 80.0 | 20.0 | 0.0 |
| EP-MC20-CF5 | 76.0 | 19.0 | 5.0 |
| EP-MC20-CF10 | 72.0 | 18.0 | 10.0 |
| EP-MC20-CF15 | 68.0 | 17.0 | 15.0 |

Scanning electron microscopy (SEM) micrographs of the cryofractured surfaces of the prepared composites were acquired using a Zeiss Supra 60 field emission scanning electron microscope (FESEM; Oberkochen, Germany), after Pt–Pd sputtering. The surface of the samples was thus coated with a nanometer layer of a metallic material to increase its electrical conductivity.

Thermogravimetric analysis (TGA) was performed with a TA Q5000IR instrument (TA Instruments, New Castle, DE). Samples of approximately 10 mg were tested at a heating rate of 10°C/min up to 700°C under a nitrogen flow of 100 mL/min. These tests allowed the measurement of the temperatures associated with a mass loss of 1% ($T_{1\%}$), the degradation temperature ($T_d$), taken as the temperature associated with the maximum mass loss rate, the total residual mass fraction ($m_r$), and the mass fraction of carbon fibers ($m_c$). Here, $m_c$ is determined from the $m_r$ values, through eq. (1):

$$m_c = m_r - m_r^{(\mathrm{E})} \times \mathrm{wt}\%^{(\mathrm{E})} \tag{1}$$

where $m_r^{(\mathrm{E})}$ is the residual mass of the sample without carbon fibers, and wt $\%^{(\mathrm{E})}$ is the weight fraction of the epoxy in the samples.

Differential scanning calorimetry (DSC) tests were performed with a Mettler DSC30 machine (Mettler Toledo, Columbus, OH) in the temperature interval between 0°C and 130°C at a heating/-cooling rate of 10°C/min under a nitrogen flow of 100 mL/min. All specimens, with a mass of approximately 10 mg each, underwent a first heating scan, a cooling scan, and a second heating scan. Through these tests, it was possible to measure the melting and crystallization temperatures ($T_m$, $T_c$) and the phase change enthalpy values ($\Delta H_m$, $\Delta H_c$) of the paraffin microcapsules and the glass-transition temperature ($T_g$) of the epoxy resin. The relative melting enthalpy values ($\Delta H_{m,\mathrm{rel}}$) were determined by dividing the $\Delta \mathrm{H_m}$ values of the composites by the $\Delta \mathrm{H_m}$ values of the neat capsules, taking into account their relative weight concentration in the composites.

Three-point flexural tests were performed according to ASTM D790 with an Instron 5969 universal testing machine (Norwood, MA) equipped with a 50 kN load cell. The nominal dimensions of the tested specimens were 70 × 10 × 3 $\mathrm{mm}^3$. The span length was fixed at 50 mm and the crosshead speed at 1.5 mm/min. At least five specimens were tested for each sample. The flexural modulus of elasticity ($E_f$), the flexural strength ($\sigma_b$), and the flexural strain at break ($\varepsilon_b$) were determined for each specimen as reported in eqs. (2), (3), and (4):

$$E_f = \frac{mL^3}{4bd^3} \tag{2}$$

$$\sigma_b = \frac{3PL}{2bd^2} \tag{3}$$

$$\varepsilon_b = \frac{6Dd}{L^2} \tag{4}$$

where $L$ is the support span, $m$ is the slope of the tangent to the initial portion of the load-deflection curve, $b$ and $d$ are the specimen width and thickness, $P$ is the maximum load, and $D$ is the deflection at the break point.

Charpy impact tests were performed at ambient temperature according to ISO 179 using a Ceast (Darmstadt, Germany) machine equipped with a hammer having a mass of 1.18 kg and setting an initial impact speed of 1 m/s. Rectangular samples of 70 × 10 × 3 $\mathrm{mm}^3$ with a notch depth of 2 mm and a notch tip radius of 0.25 mm were utilized. A span length of 62 mm was used, and at least five specimens for each sample were tested. The test allowed the measurement of the maximum force reached during the tests ($F_{\max}$), the specific energy adsorbed at the maximum load ($E_{\max}$), and the specific energy adsorbed at break ($E_{\mathrm{tot}}$).

## RESULTS AND DISCUSSION

Figure 2(a–d) shows the SEM micrographs of the composites with an MC content of 20 wt % at two different CF amounts (5 and 15 wt %). In general, it can be noticed that the capsules have a dimension between 5 and 20 μm and are homogeneously distributed within the polymer matrix. The adhesion between the epoxy and the melamine–formaldehyde shells, even though not optimal, seems rather good and comparable to that observed between the polymer matrix and the carbonaceous reinforcement. No microcapsule agglomerates can be detected, and the uniform distribution of the capsules creates a morphological continuity in the matrix, which is important for the mechanical performance of the composites. It is interesting to note that some capsules are broken. Considering that the preparation of the samples was performed under low-shear mixing conditions and that the epoxy was in the liquid state, it is reasonable to assume that the breakage of the microcapsule shells occurred during the cryofracturing operations. No substantial morphological differences can be detected by varying the CF content. The morphological features of the materials are similar to those highlighted in our previous paper on PA 12/MC blends.[9]

Table II reports the values of the theoretical density ($\rho_{\mathrm{th}}$) of the prepared samples compared with those of the experimental density ($\rho_{\mathrm{exp}}$), and their pore volume fraction ($\theta_v$). It is important to underline that for the neat epoxy sample only an experimental

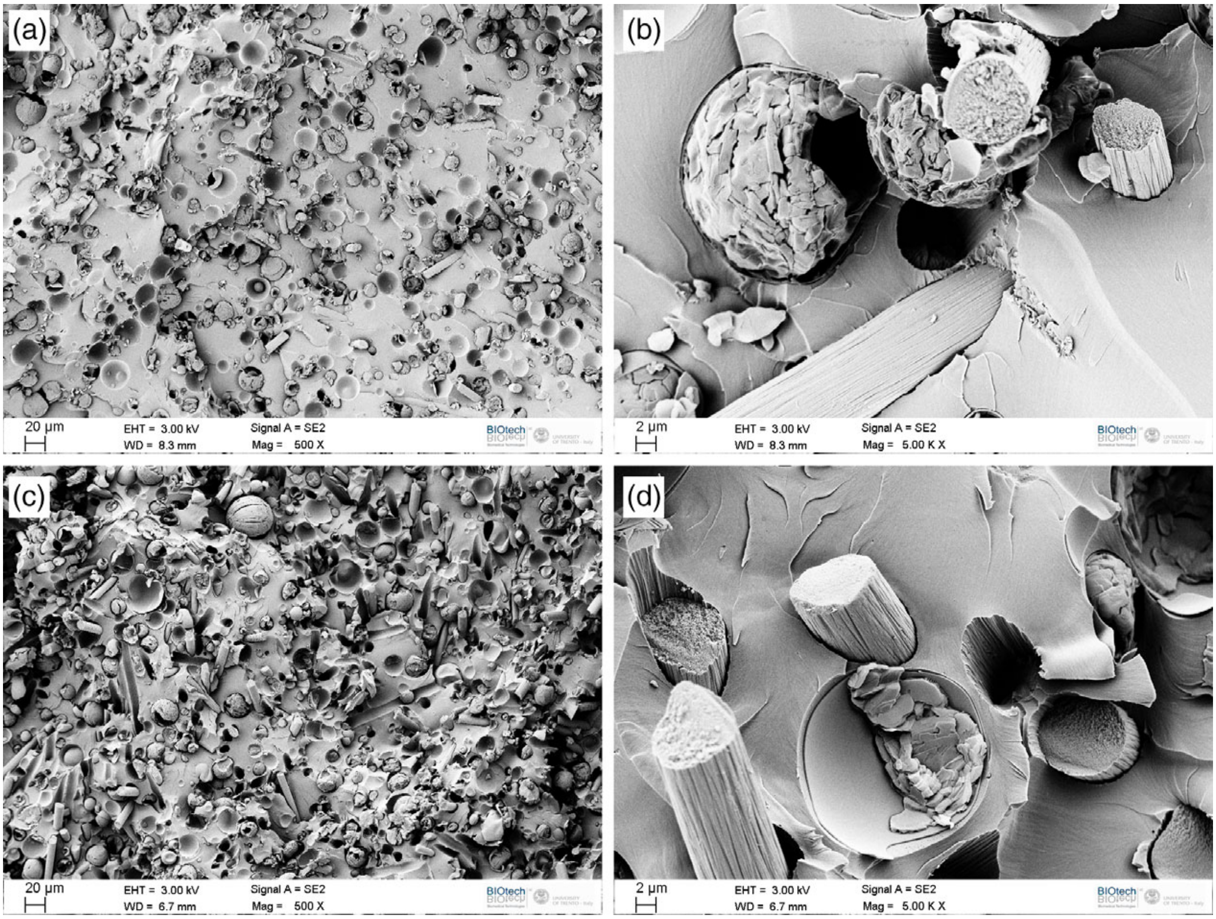

**Figure 2.** SEM micrographs of the cryofractured surfaces of the prepared composites: (a) EP-MC20-CF5, 500×; (b) EP-MC20-CF5, 5000×; (c) EP-MC20-CF15, 500×; (d) EP-MC20-CF15, 5000 × . [Color figure can be viewed at wileyonlinelibrary.com]

value can be determined (the theoretical values may depend on the base/hardener ratio and the curing conditions), and therefore the pore volume fraction was considered equal to zero (a microstructural analysis, not reported for the sake of brevity, confirmed this hypothesis). It can be noticed that the introduction of an increasing amount of MC leads to a decrease in the density values. This is not surprising since the density of MC reported by the producer is 0.90 g/cm$^3$. On the other hand, MC addition produces a progressive increase in the pore volume fraction. For instance, a $\theta_v$ value of 6.5% was determined for the EP-MC30-CF10 sample. This could negatively affect the mechanical resistance of the material, and it can be explained by considering that the introduction of MC into polymeric materials produces an increase in the viscosity, which hindered the degassing

**Table II.** Theoretical Density, Experimental Density, and Pore Volume Fraction of the Composites

| Sample | $\rho_{th}$ (g/cm$^3$) | $\rho_{exp}$ (g/cm$^3$) | $\vartheta_v$ (vol %) |
|---|---|---|---|
| EP | 1.1470[a] | 1.1470 ± 0.0014 | 0 |
| EP-CF10 | 1.2093 | 1.2005 ± 0.0002 | 0.73 ± 0.02 |
| EP-MC5-CF10 | 1.1982 | 1.1774 ± 0.0018 | 1.73 ± 0.15 |
| EP-MC15-CF10 | 1.1760 | 1.1310 ± 0.0028 | 3.82 ± 0.24 |
| EP-MC30-CF10 | 1.1426 | 1.0686 ± 0.0009 | 6.48 ± 0.08 |
| EP-MC20 | 1.0976 | 1.0573 ± 0.0014 | 3.67 ± 0.13 |
| EP-MC20-CF5 | 1.1312 | 1.0736 ± 0.0013 | 5.09 ± 0.11 |
| EP-MC20-CF10 | 1.1648 | 1.0998 ± 0.0012 | 5.58 ± 0.10 |
| EP-MC20-CF15 | 1.1985 | 1.1184 ± 0.0006 | 6.68 ± 0.05 |

Density of Et-OH 96 vol % (measured with a sphere of calibrated volume 0.71863 cm$^3$) = 0.7848 g/cm$^3$.

[a] The theoretical value was by default set equal to the experimental one.

operation and caused the presence of air bubbles in the cured composite. Similar results were also obtained in a previous work of this group,[9] in which thermoplastic composite laminates with TES capability were prepared by combining a glass fabric and a PA 12 matrix with two different PCMs, that is, the same paraffin microcapsules as used in this work, and a paraffin wax shape stabilized with carbon nanotubes. It was shown that the melt flow index (MFI) of the PA 12/PCM blends considerably decreased with the PCM concentration,[9] which is a clear indicator of a rise in viscosity. Considering the present work, the same trend in pore concentration can be seen in samples with an increasing amount of CF at a constant MC loading (20%). Also in this case, this result can be ascribed to the increase in the viscosity of the mixture.

TGA was performed to investigate trends in the thermal degradation resistance, as MC generally presents a lower thermal stability with respect to the polymer matrixes in which it is inserted. Figure 3(a,b) shows TGA thermograms of the EP-MCx-CF10 (x = 5, 10, 15) samples, and Figure 3(c,d) shows TGA curves of the EP-MCx-CF10 (x = 5, 15, 30) compositions. The most important results of the thermogravimetric analysis are summarized in Table III. It can be noticed that neat MC has a slight mass decrease at relatively low temperatures (above 150°C), followed by a more pronounced mass loss at about 420°C. Even though the temperature associated with the maximum mass loss rate of MC is higher than that shown by neat epoxy, it is confirmed that MC presents a lower thermal stability than the polymer matrix. From Table III it is interesting to note that CF introduction leads to a systematic increase in the $T_{1\%}$ values, while $T_d$ does not seem to be affected by the presence of the reinforcement. The $m_c$ values are coherent with the effective carbon fiber content in the samples. It is also worthwhile to note that the presence of CF in the composites leads to $m_r$ values higher than 10%. This result can be explained considering that CF hinders the combustion process in the polymer matrix, promoting the formation of a carbonaceous char on the surface of the materials. This behavior has been widely demonstrated in the literature, by using both microfillers and nanofillers.[53] On the other hand, the introduction of an increasing amount of MC causes a reduction in the $T_{1\%}$ parameter, and for MC contents higher than 15%, a $T_{1\%}$ value lower than that shown by the neat epoxy can be determined. At a constant MC amount of 20%, the addition of an increasing amount of CF does not seem to promote an enhancement of the thermal stability of the material, and $T_{1\%}$ and $T_d$ values lower than those shown by the EP and EP-MC20 samples

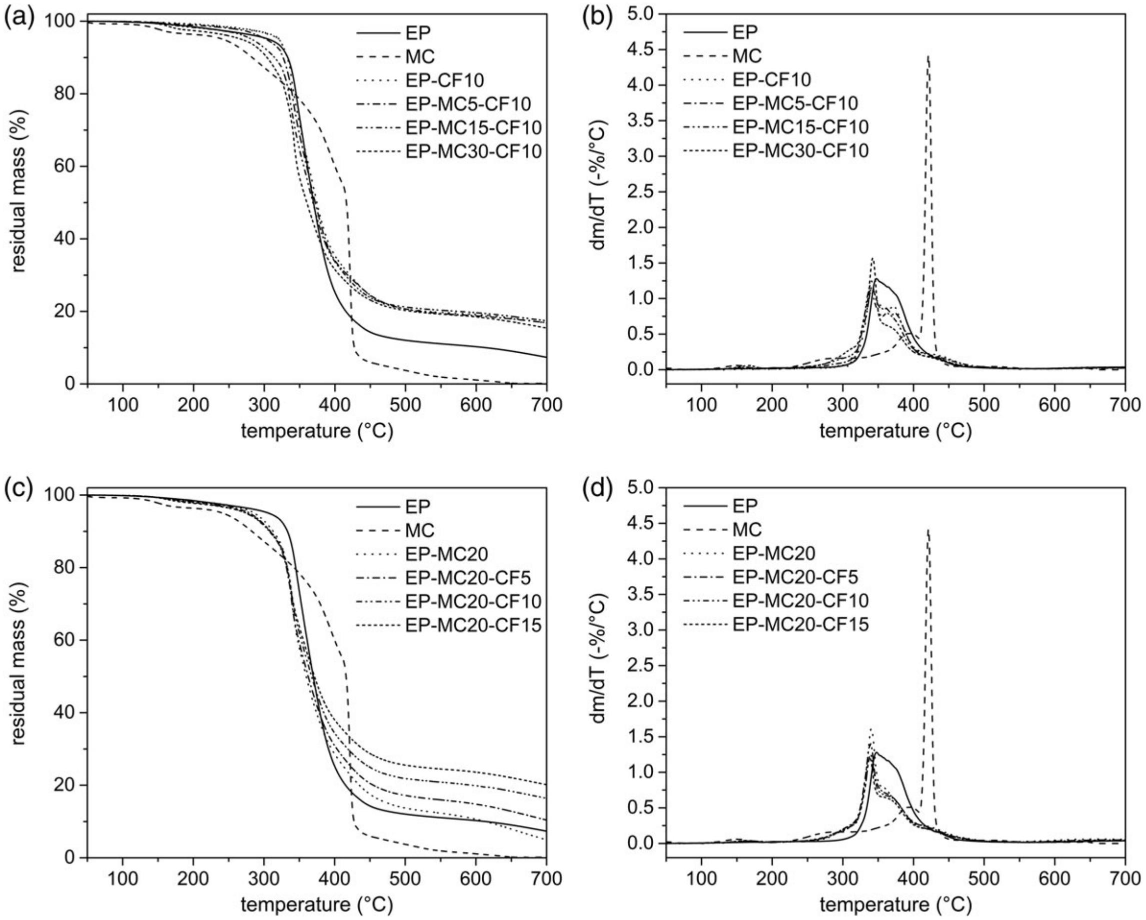

**Figure 3.** TGA thermograms of neat epoxy, neat microcapsules, and of the relative composites: (a) samples EP-MCx-CF10 (x = 5, 15, 30), mass loss as a function of temperature; (b) samples EP-MCx-CF10 (x = 5, 15, 30), derivative mass loss as a function of temperature; (c) samples EP-MC20-CFx (x = 5, 10, 15), mass loss as a function of temperature; (d) samples EP-MC20-CFx (x = 5, 10, 15), derivative mass loss as a function of temperature.

**Table III.** TGA Test Results

| Sample | $T_{1\%}$ (°C) | $T_d$ (°C) | $m_r$ (wt %) | $m_c$ (wt %) |
|---|---|---|---|---|
| EP | 171.7 | 346.7 | 7.35 | 0 |
| MC | 122.4 | 421.0 | 0.14 | 0 |
| EP-CF10 | 208.2 | 340.4 | 16.79 | 10.20 |
| EP-MC5-CF10 | 196.6 | 341.4 | 16.86 | 10.60 |
| EP-MC15-CF10 | 162.6 | 338.2 | 17.40 | 11.50 |
| EP-MC30-CF10 | 156.6 | 342.4 | 15.42 | 10.80 |
| EP-MC20 | 165.0 | 339.9 | 4.96 | 0 |
| EP-MC20-CF5 | 163.5 | 329.1 | 10.43 | 4.84 |
| EP-MC20-CF10 | 163.8 | 330.8 | 16.42 | 11.13 |
| EP-MC20-CF15 | 158.3 | 327.9 | 20.17 | 15.17 |

can be detected. Once again, at elevated CF concentrations, the formation of a carbonaceous layer within the samples is promoted, given the $m_r$ values of the EP-MC20-CF10 and EP-MC20-CF15 samples are higher than the corresponding $m_c$ values. However, it can be generally concluded that the thermal stability of the prepared composites is not seriously impaired by the presence of the microcapsules, and the temperatures at which the thermal degradation process begins are considerably above the curing and service temperatures of the epoxy resin.

The determination of the melting/crystallization behavior is fundamental to designing materials for TES applications. Therefore, DSC tests were carried out on the prepared composites. Figure 4 (a,b) shows the DSC thermograms relative to the first heating and to the cooling of the EP-MCx-CF10 (x = 5, 15, 30) samples, respectively. The data and the thermograms of the second heating scans are not reported for the sake of brevity, as no relevant differences were detected between the first and second heating scans. The main parameters measured by DSC analysis are summarized in Table IV. In the thermograms, the endothermic/exothermic peak associated with the melting/crystallization of the MC can be detected, together with an inflection point related to the glass-transition temperature ($T_g$) of the resin. The $T_g$ values do not seem to be substantially affected by the MC or CF addition and remain in the interval between 90°C and 95°C. Also, the melting ($T_m$) and crystallization ($T_c$) temperatures of the MC do not substantially change if they are inserted into the polymer matrix, and the presence of CF does not seem to influence the transition temperatures in the composites. From Table IV it can be noticed that interesting melting enthalpy values can be obtained at elevated MC concentrations. For instance, a $\Delta H_m$ value of 61 J/g was detected for the EP-MC30-CF10 composite. It is also important to underline that the $\Delta H_{m,\mathrm{rel}}$ values for all of the samples are near 100%, which confirms that the mixing and thermal curing of the composites did not cause the breakage of the capsules and underlines that the thermal energy storage/release capability of the MC is retained after the incorporation into the polymer matrixes. In a previous work of our group on PA 12/MC blends,[9] it was demonstrated that a partial breakage of the microcapsules occurred during the melt-compounding operations, thereby reducing the $\Delta H_{m,\mathrm{rel}}$ values and the TES capability of the systems. It can be hypothesized that the shear stresses generated during the compounding of a thermoplastic polymer in the molten state are more intense than those to which MC are subjected during the mixing of a thermosetting liquid resin. Therefore, it is clear that the viscosity of the polymer matrix during the production process plays a crucial role in the thermal energy storage/release capability of the resulting materials. The structural integrity of the capsules is also confirmed by the fact that the $\Delta H_c$ values detected in the cooling scan are close to the corresponding $\Delta H_m$ values measured in the first heating stage.

The mechanical behavior of the prepared composites was investigated through quasi-static flexural tests. Figure 5(a,b) shows representative load–displacement curves, and Table V summarizes the most important flexural properties. It is evident that CF addition causes an important increase in the flexural modulus ($E_f$), accompanied by a strong reduction in the strain at break ($\varepsilon_b$), as expected. For instance, for the EP-CF10 sample, an enhancement in the elastic modulus of 65% with respect to the neat epoxy can be determined, while the $\varepsilon_b$ is reduced by 50%. Moreover, the

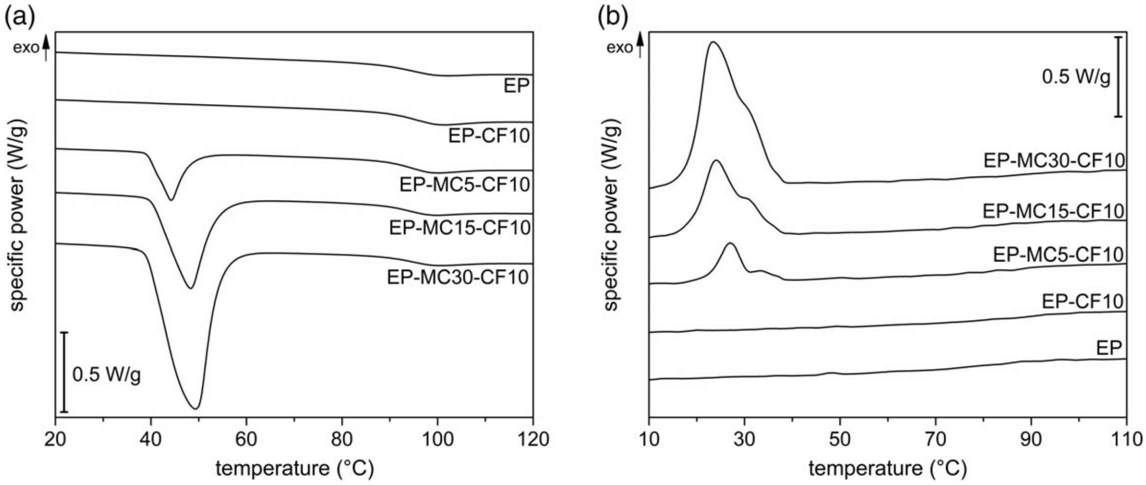

**Figure 4.** DSC thermograms of the samples EP-MCx-CF10 (x = 5, 15, 30): (a) first heating scan; (b) cooling scan.

**Table IV.** DSC Analysis Results

| Sample | $T_g$ (°C) | $T_m$ (°C) | $\Delta H_m$ (J/g) | $T_c$ (°C) | $\Delta H_c$ (J/g) |
|---|---|---|---|---|---|
| EP | 94.3 | — | — | — | — |
| MC | — | 44.1 | 200.2 | 29.6 | 198.9 |
| EP-CF10 | 94.7 | — | — | — | — |
| EP-MC5-CF10 | 93.3 | 42.8 | 10.6 | 28.2 | 10.5 |
| EP-MC15-CF10 | 92.8 | 46.5 | 29.5 | 25.8 | 29.1 |
| EP-MC30-CF10 | 93.6 | 46.4 | 60.8 | 26.2 | 60.8 |
| EP-MC20 | 95.8 | 47.8 | 47.3 | 24.2 | 46.9 |
| EP-MC20-CF5 | 92.7 | 45.7 | 43.0 | 26.7 | 42.5 |
| EP-MC20-CF10 | 90.0 | 45.9 | 40.2 | 26.3 | 39.6 |
| EP-MC20-CF15 | 90.1 | 45.0 | 39.8 | 27.8 | 39.3 |

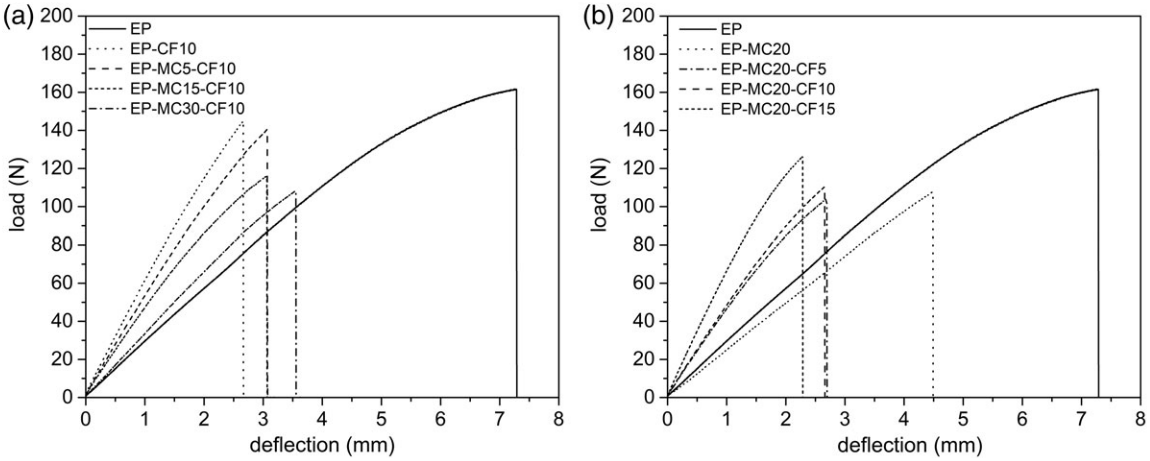

**Figure 5.** Representative load–displacement curves obtained in the three-point bending tests: (a) samples EP-MCx-CF10 (x = 5, 15, 30); (b) samples EP-MC20-CFx (x = 5, 10, 15).

stress at break ($\sigma_b$) is slightly reduced. The observed reduction of the failure properties is not surprising, since the utilized fibers are unsized. The application of a surface treatment with silane or other types of coupling agents could probably help to improve the fiber–matrix adhesion, thereby increasing the failure properties of the composites. The introduction of an increasing amount of MC causes a systematic reduction in the material stiffness, but the $E_f$ values of the EP-MC20-CF10 sample are still higher than that shown by the neat epoxy. This result is probably due to the fact that the intrinsic stiffness of the MC is much lower than that of a thermosetting matrix. In fact, in a previous work of our group[54] on thermoplastic polyurethane blends with thermal energy storage capability, it was possible to determine an elastic modulus of only 28 MPa for paraffin microcapsules, through the application of the Halphin-Tsai model. On the other hand, the failure properties are further reduced at elevated MC concentrations. As already reported in our previous work on polymer composites with TES capability,[9,48,49,55] this behavior is probably due to the nonoptimal adhesion between MC and the polymer matrixes. In these conditions, MC adds micrometer-sized defects within the materials, which lead to the premature failure of the samples. Many efforts will be devoted in the future to synthesizing surface-functionalized paraffin MC with tailored surface properties and submicrometer dimensions. Considering the mechanical properties of the EP-MC20-CFx (x = 5, 10, 15) samples, it is interesting to note that the introduction of an increasing amount of CF helps to retain the original stiffness of the material, and for the EP-MC-CF10 composite, the $E_f$ values are higher than that of the neat matrix. CF addition at elevated amounts can also increase the stress at break, limiting the $\sigma_b$ reduction by the presence of MC, while $\varepsilon_b$ values are further reduced. However, it can be concluded that MC addition

**Table V.** Main Results of the Three-Point Bending Tests

| Sample | $E_f$ (GPa) | $\sigma_b$ (MPa) | $\varepsilon_b$ (%) |
|---|---|---|---|
| EP | 2.8 ± 0.5 | 117 ± 19 | 5.1 ± 0.4 |
| EP-CF10 | 4.6 ± 0.2 | 100 ± 7 | 2.4 ± 0.2 |
| EP-MC5-CF10 | 4.1 ± 0.3 | 93 ± 2 | 2.5 ± 0.3 |
| EP-MC15-CF10 | 3.9 ± 0.2 | 77 ± 2 | 2.4 ± 0.1 |
| EP-MC30-CF10 | 3.6 ± 0.1 | 60 ± 1 | 2.0 ± 0.1 |
| EP-MC20 | 2.0 ± 0.4 | 52 ± 3 | 3.1 ± 0.2 |
| EP-MC20-CF5 | 2.5 ± 0.2 | 53 ± 2 | 2.6 ± 0.3 |
| EP-MC20-CF10 | 3.5 ± 0.2 | 60 ± 7 | 2.0 ± 0.2 |
| EP-MC20-CF15 | 4.5 ± 0.3 | 72 ± 2 | 2.0 ± 0.1 |

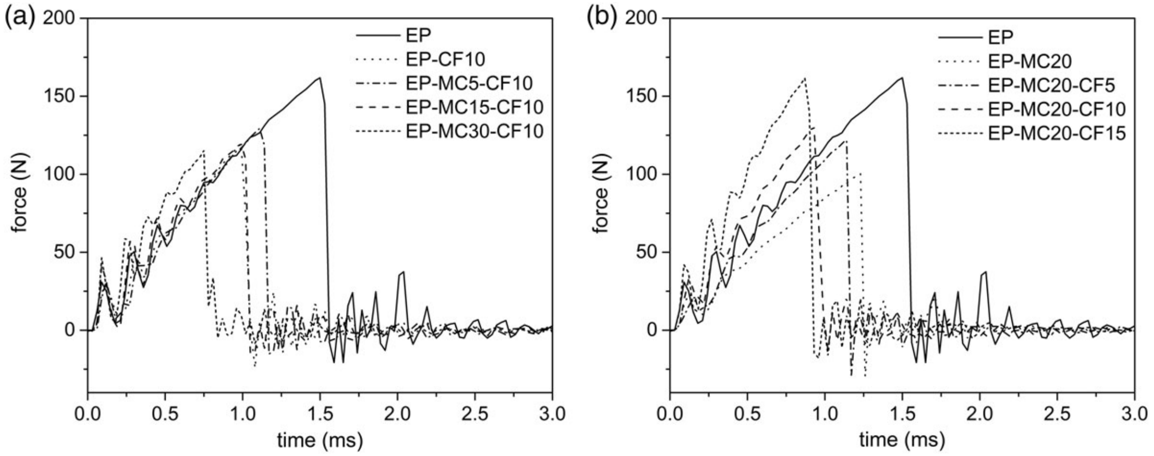

**Figure 6.** Representative load–time curves obtained in the Charpy impact tests: (a) samples EP-MCx-CF10 (x = 5, 15, 30); (b) samples EP-MC20-CFx (x = 5, 10, 15).

does not dramatically deteriorate the flexural properties of the samples, and the presence of CF positively contributes to the material stiffness and strength. It is also important to underline that the presence of CF within the materials could also increase their thermal conductivity, thereby leading to a more efficient heat diffusion within the material. Thermal conductivity tests will be carried out in the future on these samples to verify this hypothesis.

One of the main drawbacks related to the use of epoxy resins is their intrinsic brittleness under impact conditions. Therefore, it could be important to evaluate the effect of CF and MC addition with Charpy impact tests. In Figure 6(a,b), representative load–time curves of the prepared materials are reported, and the most important results are collected in Table VI. The introduction of CF within the epoxy causes a slight decrease in the maximum force (it should be noted that all of the samples have the same dimensions) and of both the $E_{max}$ and $E_{tot}$ values. Once again, this is probably due to nonoptimal fiber–matrix interfacial adhesion. It is interesting to note that the addition of an increasing concentration of MC does not lead to substantial variations in $F_{max}$, while both $E_{max}$ and $E_{tot}$ parameters are even higher than those displayed by the EP-CF10 sample. These results can be explained by considering the plasticizing role played by paraffin microcapsules within the material under impact conditions. On the other hand, the impact properties displayed by the EP-MC20 sample are lower than those of the neat matrix, but the addition of an increasing CF loading causes an increase in the $F_{max}$ values up to a level comparable to that of the neat epoxy, and the $E_{max}$ and $E_{tot}$ values are also slightly improved. As reported for flexural tests, it can be generally concluded that the reduction in the impact properties of the prepared composites is not dramatic, and the presence of CF helps to increase the impact resistance of the materials.

**Table VI.** Charpy Impact Test Results

| Sample | $F_{max}$ (N) | $E_{max}$ (kJ/m$^2$) | $E_{tot}$ (kJ/m$^2$) |
|---|---|---|---|
| EP | 138 ± 52 | 3.5 ± 0.3 | 3.6 ± 2.3 |
| EP-CF10 | 110 ± 22 | 1.6 ± 0.6 | 1.7 ± 0.6 |
| EP-MC5-CF10 | 131 ± 3 | 2.7 ± 0.2 | 3.0 ± 0.5 |
| EP-MC15-CF10 | 123 ± 5 | 2.5 ± 0.2 | 2.5 ± 0.2 |
| EP-MC30-CF10 | 116 ± 13 | 1.7 ± 0.2 | 1.8 ± 0.1 |
| EP-MC20 | 97 ± 10 | 1.6 ± 0.5 | 1.7 ± 0.5 |
| EP-MC20-CF5 | 126 ± 19 | 2.0 ± 0.5 | 2.2 ± 0.4 |
| EP-MC20-CF10 | 132 ± 6 | 1.8 ± 0.2 | 1.9 ± 0.1 |
| EP-MC20-CF15 | 163 ± 9 | 2.0 ± 0.1 | 2.2 ± 0.1 |

## CONCLUSIONS

The presented work concerns the preparation and characterization of multifunctional epoxy–short carbon fiber composites having thermal energy storage/release capability, obtained by adding paraffin microcapsules and CF at different relative concentrations to an epoxy matrix. A uniform distribution of the capsules within the matrix, with a rather good interfacial adhesion, was observed through SEM images, while the increase in the void volume fraction detected by density measurements was probably due to the increase of the polymer viscosity at elevated CF or MC amounts. Noteworthy melting enthalpy values (up to 60 J/g) were obtained at elevated MC concentrations, which indicates that the production process of the composites did not cause capsule breakage or paraffin leakage out of the composite. The thermal stability of the samples was not remarkably compromised by MC introduction, given that the service temperature of the material is far above the level at which the thermal degradation of the capsules occurs. MC addition decreased the mechanical properties of the samples, while CF introduction positively contributed to the material stiffness and strength. This work demonstrated the possibility of developing novel multifunctional carbon fiber reinforced composites combining thermal energy storage/release capability and good thermomechanical properties.

## REFERENCES

1. Kalaiselvam, S.; Parameshwaran, R. Thermal Energy Storage Technologies for Sustainability; Elsevier: Amsterdam, Netherlands, **2014**; Chapter 5.

2. Kenisarin, M. M.; Kenisarina, K. M. *Renew. Sustain. Energy Rev.* **2012**, *16*, 1999.
3. Pielichowska, K.; Pielichowski, K. *Prog. Mater. Sci.* **2014**, *65*, 67.
4. Farid, M. M.; Khudhair, A. M.; Razack, S. A. K.; Al-Hallaj, S. *Energ. Conver. Manage.* **2004**, *45*, 1597.
5. Wang, Z. Y.; Qiu, F.; Yang, W. S.; Zhao, X. D. *Renew. Sustain. Energy Rev.* **2015**, *52*, 645.
6. Khudhair, A. M.; Farid, M. M. *Energ. Conver. Manage.* **2004**, *45*, 263.
7. Kuznik, F.; David, D.; Johannes, K.; Roux, J. J. *Renew. Sustain. Energy Rev.* **2011**, *15*, 379.
8. Juozapaitis, A.; Vainiūnas, P.; Zavadskas, E. K.; Ostry, M.; Charvat, P. *Procedia Eng.* **2013**, *57*, 837.
9. Fredi, G.; Dorigato, A.; Pegoretti, A. *eXPRESS Polym. Lett.* **2018**, *12*, 349.
10. Hasnain, S. M. *Energ. Conver. Manage.* **1998**, *39*, 1127.
11. Himran, S.; Suwono, A.; Mansoori, G. A. *Energy Source.* **1994**, *16*, 117.
12. Trigui, A.; Karkri, M.; Boudaya, C.; Candau, Y.; Ibos, L.; Fois, M. *J. Compos. Mater.* **2014**, *48*, 49.
13. Akgün, M.; Aydın, O.; Kaygusuz, K. *Energ. Conver. Manage.* **2007**, *48*, 669.
14. Jeong, S.-G.; Kim, S.; Huh, W. *J. Adhes. Sci. Technol.* **2014**, *28*, 711.
15. Cui, Y.; Xie, J.; Liu, J.; Pan, S. *Procedia Eng.* **2015**, *121*, 763.
16. Dorigato, A.; Ciampolillo, M. V.; Cataldi, A.; Bersani, M.; Pegoretti, A. *Rubber Chem. Technol.* **2017**, *90*, 575.
17. Shin, Y.; Yoo, D. I.; Son, K. *J. Appl. Polym. Sci.* **2005**, *96*, 2005.
18. Kürklü, A.; Özmerzi, A.; Bilgin, S. *Renew. Energy.* **2002**, *26*, 391.
19. Cabeza, L. F.; Ibáñez, M.; Solé, C.; Roca, J.; Nogués, M. *Appl. Therm. Eng.* **2006**, *26*, 1328.
20. Wirtz, R.; Fuchs, A.; Narla, V.; Shen, Y.; Zhao, T.; Jiang, Y. 41st Aerospace Sciences Meeting and Exhibit, Aerospace Sciences Meetings, **2003**, https://doi.org/10.2514/6.2003-513.
21. Sharma, R. K.; Ganesan, P.; Tyagi, V. V.; Metselaar, H. S. C.; Sandaran, S. C. *Energ. Conver. Manage.* **2015**, *95*, 193.
22. Luyt, A. S.; Krupa, I. *Energ. Conver. Manage.* **2009**, *50*, 57.
23. Mu, M. L.; Basheer, P. A. M.; Sha, W.; Bai, Y.; McNally, T. *Appl. Energy.* **2016**, *162*, 68.
24. Sari, A.; Akcay, M.; Soylak, M.; Onal, A. *J. Sci. Ind. Res.* **2005**, *64*, 991.
25. Sobolciak, P.; Karkri, M.; Al-Maaded, M. A.; Krupa, I. *Renew. Energy.* **2016**, *88*, 372.
26. Zhang, P.; Hu, Y.; Song, L.; Ni, J.; Xing, W.; Wang, J. *Solar Energy Mater. Solar Cells.* **2010**, *94*, 360.
27. Dorigato, A.; Canclini, P.; Unterberger, S. H.; Pegoretti, A. *eXPRESS Polym. Lett.* **2017**, *11*, 738.
28. Mehrali, M.; Latibari, S. T.; Mehrali, M.; Mahlia, T. M. I.; Metselaar, H. S. C. *Energ. Conver. Manage.* **2014**, *88*, 206.
29. Sari, A.; Soylak, M. *J. Serb. Chem. Soc.* **2007**, *72*, 485.
30. Chen, Y. M.; Luo, W.; Wang, J.; Huang, J. *J. Phys. Chem. C.* **2017**, *121*, 12603.
31. Huang, X.; Lin, Y. X.; Alva, G.; Fang, G. Y. *Solar Energy Mater. Solar Cells.* **2017**, *170*, 68.
32. Khadiran, T.; Hussein, M. Z.; Zainal, Z.; Rusli, R. *Solar Energy Mater. Solar Cells.* **2015**, *143*, 78.
33. Onder, E.; Sarier, N.; Cimen, E. *Thermochim. Acta.* **2008**, *467*, 63.
34. Su, J. F.; Wang, X. Y.; Wang, S. B.; Zhao, Y. H.; Zhu, K. Y.; Yuan, X. Y. *Polym. Compos.* **2011**, *32*, 810.
35. Carlson, T. PhD dissertation, Department of Engineering Sciences and Mathematics, Materials Science, Luleå University of Technology, Luleå, Sweden, **2013**.
36. Gibson, R. F. *Compos. Structures.* **2010**, *92*, 2793.
37. Salonitis, K.; Pandremenos, J.; Paralikas, J.; Chryssolouris, G. *Int. J. Adv. Manuf. Technol.* **2010**, *49*, 803.
38. Christodoulou, L.; Venables, J. D. *JOM.* **2003**, *55*, 39.
39. Friedrich, K. In Multifunctionality of Polymer Composites: Challenges and New Solutions; K. Friedrich and U. Breuer, Eds., Elsevier: Waltham, MA, USA, **2015**. pp. 3–41.
40. Kastiukas, G.; Zhou, X. M.; Castro-Gomes, J. *Construct. Build Mater.* **2016**, *110*, 201.
41. Su, J. F.; Zhao, Y. H.; Wang, X. Y.; Dong, H.; Wang, S. B. *Part A.* **2012**, *43*, 325.
42. Wang, X. Y.; Su, J. F.; Wang, S. B.; Zhao, Y. H. *Polym. Compos.* **2011**, *32*, 1439.
43. Zhang, P.; Xiao, X.; Ma, Z. W. *Appl. Energy.* **2016**, *165*, 472.
44. Ozaki, T.; Takeya, H.; Kume, M.; Sekine, K. *SAMPE J.* **2008**, *44*, 6.
45. Silverman, E. *SAMPE J.* **2005**, *41*, 19.
46. Yoo, S.; Kandare, E.; Shanks, R.; Al-Maadeed, M. A.; Afaghi Khatibi, A. *Thermochim. Acta.* **2016**, *642*, 25.
47. Yoo, S.; Kandare, E.; Shanks, R.; Khatibi, A. A. Presented at the International Conference of Materials Processing and Characterization (ICPMC), Hyderabad, India, **2017**.
48. Fredi, G.; Dorigato, A.; Fambri, L.; Pegoretti, A. *Polymers.* **2017**, *9*, 405.
49. Fredi, G.; Dorigato, A.; Fambri, L.; Pegoretti, A. *Compos. Sci. Technol.* **2018**, *158*, 101.
50. Rezaei, F.; Yunus, R.; Ibrahim, N. A. *Mater. Design.* **2009**, *30*, 260.
51. Zhang, H.; Zhang, Z.; Friedrich, K. *Compos. Sci. Technol.* **2007**, *67*, 222.
52. ASTM D792-13, Standard Test Methods for Density and Specific Gravity (Relative Density) of Plastics by Displacement, ASTM International, West Conshohocken, PA, **2013**.
53. Dorigato, A.; Pegoretti, A.; Frache, A. *J. Therm. Anal. Calorim.* **2012**, *109*, 863.
54. Dorigato, A.; Rigotti, D.; Pegoretti, A. *Front. Mater.* **2018**, *5*, 58.
55. Rigotti, D.; Dorigato, A.; Pegoretti, A. *Mater. Today Commun.* **2018**, *15*, 228.